

Sliding Mode Control of Lateral Motion for Four Driving-Steering Wheels Autonomous Vehicle

Bogdan Dumitrașcu*, Adrian Filipescu*

* Department of Automation and Electrical Engineering University "Dunarea de Jos" of Galati, Galati, Romania (e-mail :dumi_b20@yahoo.com, Adrian.Filipescu@ugal.ro)

Abstract: The sliding-mode controller (SMC) for the lateral motion control problem of Four Driving-Steering Wheels (4DW/SW) vehicle is presented in this paper. The lane centerline tracking is the main control performance. The dynamic model of the vehicle has been taken into account. Closed-loop robustness to uncertainties is achieved. The lane centerline tracking is achieved using look-ahead techniques. Closed-loop simulation and real time results with 4DW/SW SEEKUR robot base show the efficiency of sliding-mode control. Compared to 2DW and one or two SW mobile robots control, the 4DW/SW sliding-mode control is more stable with smaller lateral error.

Keywords: Sliding Mode Control, Autonomous Vehicle, Computer Control, Four Wheel Drive/Steering.

1. INTRODUCTION

The control of non-holonomic vehicles has been a very active research field, for many years. There are several reasons for this fact. One reason is the fact that wheeled vehicles constitute a major and ever more omnipresent transportation system. The progress of research and technology allows previously restricted to research laboratories and factories, automated wheeled vehicles to be envisioned in everyday life (e.g. through carplatooning applications or urban transportation services), not to mention the military domain.

Autonomous vehicle control can be divided in two control tasks. The first task, longitudinal control, involves controlling the vehicle speed to maintain a proper spacing between vehicles.

The second task, lateral control, is concerned with automatic steering of vehicles for lane tracking in order to follow a reference along the lane center. This paper concentrates on the lateral control task.

Steering control of vehicles has been studied since late 1950's. Steering control problem requires addressing two parts: sensing and control (Hiraoka *et al.*, 2009; She *et al.*, 2007; Abdullah *et al.*, 2006). Steering control approaches can be grouped into look-ahead and look-down systems. Look-ahead systems replicate human driving behavior by measuring the lateral error ahead of the vehicle. A number of research groups have successfully conducted highway speed experiments with look-ahead systems like machine vision and laser. Another approach is the look-down system which measures the lateral displacement at a location within or in the close vicinity of vehicle boundaries, typically straight down the front bumper.

Look-ahead systems replicate human driving behaviour by measuring the lateral displacement ahead of the vehicle. The look-ahead distance usually is increased with increasing velocity, similar to human behaviour. This paper deals with the kinematics and dynamics models and the feedback control of an autonomous wheeled robot named SEEKUR (Fig.1) from the Mobile Robots Inc.



Fig. 1. SEEKUR robot base ground vehicle.

Outdoor robots face all of the same challenges as indoor robots, such as sensing, data processing, locomotion, navigation, and interaction with the surroundings. Outdoor robots, however, are expected to achieve all of these things in much more complex and unstructured environments such as forests, deserts, and even agricultural fields (Huntsberger *et al.*, 2002; Lacaze *et al.*, 2002; Montemerlo *et al.*, 2006; Wellington *et al.*, 2004).

Variable structure control (VSC) has been showing to be a robust approach in different applications and has been successfully applied in control problems as diverse as automatic flight control, control of electric motors, regulation in chemical processes, helicopter stability augmentation, space systems and robotics. One particular type of VCS system is the sliding mode control (SMC) methodology (Utkin, 1992). The theory of SMC has been applied to various control systems, since it has been shown that this nonlinear type of control exhibits some excellent properties, such as robustness against large parameter variation and disturbances (Utkin *et al.*, 1999; Slotine and Li, 1991; Solea *et al.*, 2009a, c; Solea, 2009b). By designing switch functions of state variables or output variables to form sliding surfaces, SMC can guarantee that when trajectories reach the surfaces, the switch functions keep the trajectories on the surfaces, thus yielding the desired system dynamics. The main advantages of using SMC include fast response, good transient and robustness with respect to system uncertainties and external disturbances.

2. LATERAL CONTROL PROBLEM FOR VEHICLES

The control objective in lateral control of vehicles for lane tracking can be seen as keeping the distance of a point(or its vertical projection on the road) to the road centerline zero.

The vehicle model for control design and control objective is described in the following subsection.

2.1. Vehicle Model

Table 1. Reference Vehicle Parameters

Parameter	Value
Vehicle mass (m)	350 kg
Yaw moment of inertia (I_ψ)	725 kg * m ²
Front axle to CG length (l_f)	0.70 m
Rear axle to CG length (l_r)	0.70 m
Front cornering stiffness (C_f)	17.000 N/rad
Rear cornering stiffness (C_r)	17.000 N/rad

A complex vehicle model includes six degrees of freedom for the vehicle sprung mass, four wheel states, and two engine states. Additionally, the brake, throttle, and steering actuators are modelled as linear first-order systems. The suspension system is modelled as four independent spring-damper systems. From the complex model, we derive the simplified model to design a sliding-mode controller under the following assumptions: the roll, pitch and vertical motion are neglected; the normal forces acting on tires are approximated as static values; the actuator dynamics for brake, throttle and steering are discounted.

For a linear 2 DOF bicycle mode (Fig. 2), when the front and rear steering angles δ_f and δ_r are small, the lateral

velocity (v_y) and yaw moment ($r = \dot{\psi}$) are described by the following equation:

$$\begin{bmatrix} \dot{v}_y \\ \dot{r} \end{bmatrix} = \begin{bmatrix} a_{11} & a_{12} \\ a_{21} & a_{22} \end{bmatrix} \cdot \begin{bmatrix} v_y \\ r \end{bmatrix} + \begin{bmatrix} b_{11} & b_{12} \\ b_{21} & b_{22} \end{bmatrix} \cdot \begin{bmatrix} \delta_f \\ \delta_r \end{bmatrix} \quad (1)$$

where:

$$\begin{cases} a_{11} = -\frac{C_f + C_r}{m \cdot v_x} & b_{11} = \frac{C_f}{m} \\ a_{12} = \frac{-l_f \cdot C_f + l_r \cdot C_r}{m \cdot v_x} & b_{12} = \frac{C_r}{m} \\ a_{21} = \frac{-l_f \cdot C_f + l_r \cdot C_r}{I_\psi \cdot v_x} & b_{21} = \frac{l_f \cdot C_f}{I_\psi} \\ a_{22} = \frac{l_f^2 \cdot C_f + l_r^2 \cdot C_r}{I_\psi \cdot v_x} & b_{22} = \frac{l_r \cdot C_r}{I_\psi} \end{cases} \quad (2)$$

with parameters defined as: m - total vehicle mass, I_ψ - total vehicle inertia about vertical axis at CG [$kg \cdot m^2$], l_f (l_r) - distance of front(rear) axle from CG, C_f (C_r) - front (rear) tire cornering stiffness [N/rad], v_x (v_y) - longitudinal (lateral) velocity [m/s], δ_f (δ_r) - front (rear) wheel steer angle [rad], r - yaw rate [rad/s], CG - centre of gravity (see Table 1).

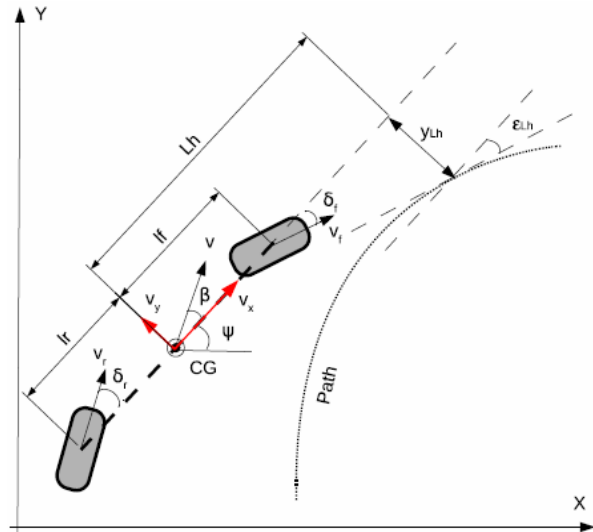


Fig. 2. Linear 2 DOF bicycle mode

Two special maneuvers, the so-called Zero-side-slip Maneuver and Parallel Steering Maneuver (Danwei and Feng, 2001), take advantage of the special kinematic characteristic of 4 DW/SW vehicles and are commonly used. In the following, we will show how these two maneuvers can be used in our problem.

- A. Zero-side-slip Maneuver - In this maneuver, the sideslip angle is set to zero from the starting point to the ending point when the vehicle moves along the path. The orientation of the vehicle $\psi(t)$ is set to match the tangential angle of the desired path $\psi_d(t)$. This maneuver is desirable in vehicle motion since

the vehicle body is always tangent to the path (see Fig. 3A).

B. Parallel Steering Maneuver - Parallel Steering is defined as that both two wheels are always steered at the same angle in the same direction. In this maneuver, two steering angles is set as follows $\delta_f(t) = \delta_r(t), t = 0 \rightarrow t_{fin}$. This implies that the vehicle translates without changing its orientation during the motion. Thus we have $\psi(t) = \psi_0, t = 0 \rightarrow t_{fin}$ where ψ_0 is the initial heading angle of the vehicle. This maneuver is very practical in vehicle lanechanging and obstacle avoidance (see Fig. 3B). The rotation of the vehicle is reduced as well, thus improves the vehicle stability at high speed.

In this paper is taken into account first case (case A) where $\delta_r = -\delta_f$.

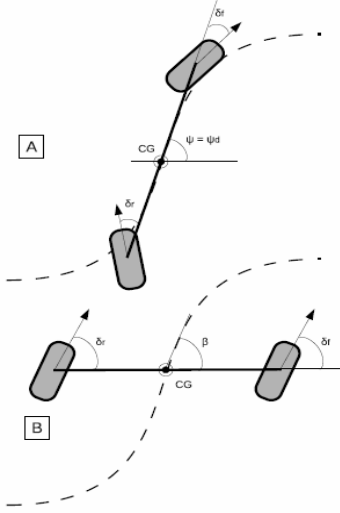


Fig. 3. A. Zero-side-slip maneuver and B. Parallel steering maneuver.

The model described by (1) is independent of the road reference. To describe the vehicle relative to the road, the vision dynamics of the system is modelled using visual information and road geometry. Figure 2 shows a vehicle following a desired path with road curvature K . In this paper, the vehicle is assumed to be equipped with a set of vision system. The vision system is used to estimate the offset from the centerline y_{Lh} and angle between the road tangent and heading of the vehicle ε_{Lh} at some look-ahead distance Lh where measurement is taken.

The equations capturing the evolution of these measurements due to the motion of the vehicle and changes in the road geometry are:

$$\begin{cases} \dot{y}_{Lh} = v_x \cdot \varepsilon_{Lh} - v_y - r \cdot Lh \\ \dot{\varepsilon}_{Lh} = v_x \cdot K - r \end{cases} \quad (3)$$

The main characteristics that must rule the lateral control and that differentiate it from trajectory tracking (TT), can be summarized as follows:

- Only the global shape of the path is considered to do the following. The desired trajectory evolution (governed by time) must not play any role in the track as it does in TT.
- The existence of the rigid law in TT means pulling or dragging the robot to reach the reference. On the other hand, in lateral control the reference path can not pull (or drag) the robot: the robot must move independently by some condition (of course, meanwhile a control law must ensure convergence to the path). We must impose a motion in the real system to guarantee that it moves or progresses. In the current mobile robot literature most motion exigencies are applied to mobile robots, so it is usual to have $v_{xd} = ct$ (other authors use $|v_{xd}| \neq 0$) or a velocity profile for v_{xd} is supposed to be given between the initial and final position.
- A direct result of what is explained before is that there is no time exigency in the lateral control. This means that we cannot ensure that the robot will reach a reference point in a predictable period of time.

3. SLIDING-MODE CONTROLLER

A Sliding Mode Controller is a Variable Structure Controller (VSC). Basically, a VSC includes several different continuous functions that map plant state to a control surface, and the switching among different functions is determined by plant state that is represented by a switching function.

Gao and Hung (1993) proposed a method of reaching mode and reaching law, based on m -input n th-order systems. In order to assure the attraction of state trajectory onto the switching manifold within the reaching mode, they suggested the control of reaching speed by certain reaching law. The general form of reaching law is:

$$\dot{s} = -Q \cdot \text{sgn}(s) - P \cdot h(s) \quad (4)$$

where

$$\begin{aligned} Q &= \text{diag}[q_1, q_2, \dots, q_m]; q_i > 0 \\ \text{sgn}(s) &= [\text{sgn}(s_1), \text{sgn}(s_2), \dots, \text{sgn}(s_m)]^T \\ P &= \text{diag}[p_1, p_2, \dots, p_m]; p_i > 0 \\ h(s) &= [h_1(s_1), h_2(s_2), \dots, h_m(s_m)]^T \\ s_i * h_i(s_i) &> 0; h_i(0) = 0 \end{aligned}$$

A practical form of reaching the control law is defined as

$$\dot{s} = -Q \cdot \text{sgn}(s) - P \cdot s \quad (5)$$

This reaching law increases the reaching speed when the state is far away from the switching manifold, but reduces the rate when the state is near the manifold. The result is a fast reaching and low chattering reaching mode. In addition, because of the absence of the $-Q \cdot \text{sgn}(s)$ term on the righthand side of (4), this reaching law eliminates the chattering.

A new design of sliding surface is proposed such that lateral error, y_{Lh} , and angular error, ε_{Lh} , are internally coupled with each other in a sliding surface leading to convergence of both variables. For that purpose the following sliding surface was proposed:

$$s = \dot{y}_{Lh} + \gamma_y \cdot y_{Lh} + \gamma_0 \cdot \text{sgn}(y_{Lh}) \cdot |\varepsilon_{Lh}| \quad (6)$$

here γ_0 and γ_y are positive constant parameters.

If s converges to zero, in steady-state it becomes

$$\dot{y}_{Lh} = -\gamma_y \cdot y_{Lh} - \gamma_0 \cdot \text{sgn}(y_{Lh}) \cdot \varepsilon_{Lh}. \quad (7)$$

For $y_{Lh} < 0 \Rightarrow \dot{y}_{Lh} > 0$. For $y_{Lh} > 0 \Rightarrow \dot{y}_{Lh} < 0$. Finally, it can be known from s that the convergence of y_{Lh} and \dot{y}_{Lh} leads to the convergence of ε_{Lh} to zero.

From the time derivative of (6) and using the reaching law defined in (5) yields:

$$\begin{aligned} \dot{y} &= \ddot{y}_{Lh} + \gamma_y \cdot \dot{y}_{Lh} + \gamma_0 \cdot \text{sgn}(y_{Lh}) \cdot \text{sgn}(\varepsilon_{Lh}) \cdot \dot{\varepsilon}_{Lh} = \\ &= -Q \cdot \text{sgn}(s) - P \cdot s \end{aligned} \quad (8)$$

From (1), (3), (8) and after some mathematical manipulation, we get the output command of the sliding-mode controller:

$$\delta_{fc} = \frac{Q \cdot \text{sgn}(s) + P \cdot s + \gamma_y \cdot \dot{y}_{Lh} + E}{b_{11} + b_{12} + (b_{21} + b_{22}) \cdot Lh} \quad (9)$$

where

$$\begin{aligned} E &= \dot{v}_x \cdot \varepsilon_{Lh} + v_x \cdot \dot{\varepsilon}_{Lh} - v_y \cdot (a_{11} + a_{21} \cdot Lh) - \\ &- r \cdot (a_{12} + a_{22} \cdot Lh) + \gamma_0 \cdot \text{sgn}(y_{Lh} \cdot \varepsilon_{Lh}) \cdot \dot{\varepsilon}_{Lh} \end{aligned} \quad (10)$$

4. SIMULATION RESULTS

In this section, some simulation results are presented to validate the proposed control law. To show the effectiveness of the proposed sliding mode control law numerically, experiments were carried out on the lateral control problem of a 4 DW/SW vehicle. The DW/SW vehicle is assumed to have the same structure as in Fig. 2.

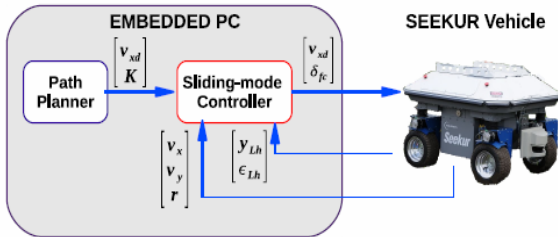


Fig. 4. Sliding-mode control architecture.

The 4 DW/SW vehicle has a two-level control architecture(see Fig.4). High-level control algorithms are written in C++ and run with a sampling time of $T_s=100$ ms on an embedded PC, which also provides interface with real-time visualisation and a simulation environment.

All the simulations were made using the MobileSim. MobileSim is software for simulating MobileRobots' platforms and their environments, for debugging and experimentation with ARIA. The ARIA software can be used to control the mobile robots like Pioneer, PatrolBot, PeopleBot, Seekur etc. ARIA (Advanced Robot Interface for Applications) it is an object-oriented Applications Programming Interface (API), written in C++ and intended for the creation of intelligent high-level client-side software.

Two simulation experiments were carried out to evaluate the performance of the sliding mode controller presented in Section III. The first simulation refers to the case of circular path ($v_{xd} = 0.5m/s$ and $K = 0.2$). The look-ahead distance is $Lh = 1m$.

In the second simulation the 4 DW/SW robot execute a linear path ($v_{xd} = 0.5m/s$ and $K = 0$).

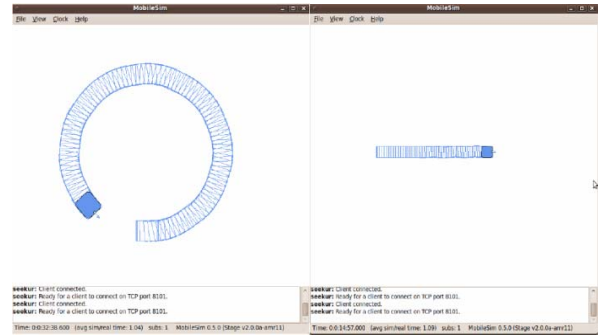


Fig. 5. Simulation results using Aria and MobileSim software (case I and II).

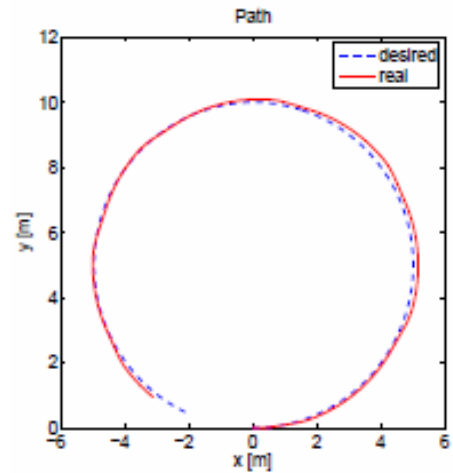


Fig. 6. Simulation I - 4WDS robot made a circular path

Fig. 6 shows the trajectory of the 4 DW/SW robot when the robot executes a circular path. In Fig. 7 the sliding surface s and steering command (δ_f) are shown. Finally, Figs. 8 show the time histories of the offset from the centerline at the look-ahead (y_{Lh}) and the angle between the tangent to the road and the vehicle orientation (ε_{Lh}).

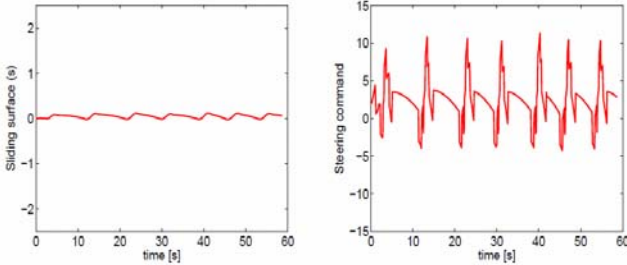


Fig. 7. Simulation I - Sliding surface (s) and the steering command (δ_f).

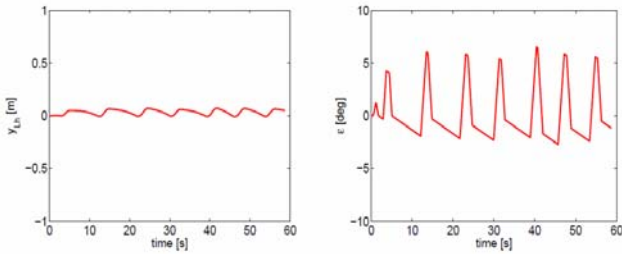


Fig. 8. Simulation I - Variation of the offset from the centerline at the look-ahead (y_{Lh}) and the angle between the tangent to the road and the vehicle orientation (ε_{Lh}).

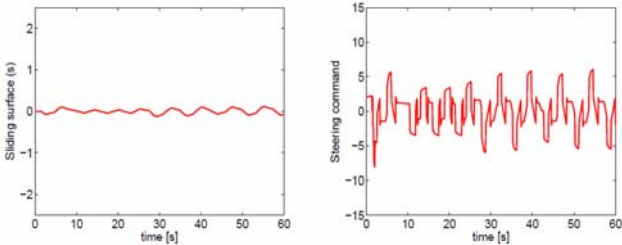


Fig. 9. Simulation II - Sliding surface (s) and the steering command (δ_f).

In Fig. 9 the sliding surface s and steering command (δ_f) are shown, when 4 DW/SW vehicle execute a linear path.

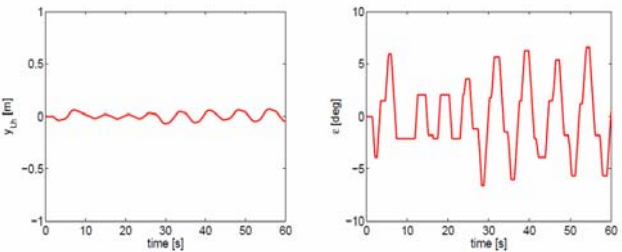


Fig. 10. Simulation II - Variation of the offset from the centerline at the look-ahead (y_{Lh}) and the angle between the tangent to the road and the vehicle orientation (ε_{Lh}).

In Figs. 10 are shown the time histories of the offset from the centerline at the look-ahead (y_{Lh}) and the angle between the tangent to the road and the vehicle orientation (ε_{Lh}).

5. REAL TIME RESULTS

In this section, test results are presented to validate the proposed control law. To show the effectiveness of the proposed sliding mode control law, experiments were carried out on the lateral control problem of a Seekur vehicle.

The high-level control algorithms (including desired motion generation) are written in C++ and run with a sampling time of $T_s = 100$ ms on a PC. A wireless network was set in order to allow data transfer between the robot and the PC. The wireless network used a wireless access point and an universal device server that was connected to the access point and the serial connector of the robot.

An experiment was carried out to evaluate the performance of the sliding mode controller presented in Section III. The test refers to the case of linear path ($v_{xd} = 0.3m/s$ and $K = 0.2$).

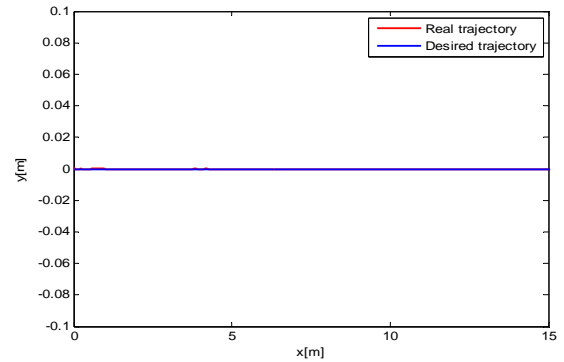


Fig. 11. Real time trajectory of a Seekur robot.

Fig. 11 shows the trajectory of the 4 DW/SW robot when the robot executes a linear path. In Fig. 12 the sliding surface s and steering command (δ_f) are shown. Finally, Figs. 13 show the time histories of the offset from the centerline at the look-ahead (y_{Lh}) and the angle between the tangent to the road and the vehicle orientation (ε_{Lh}).

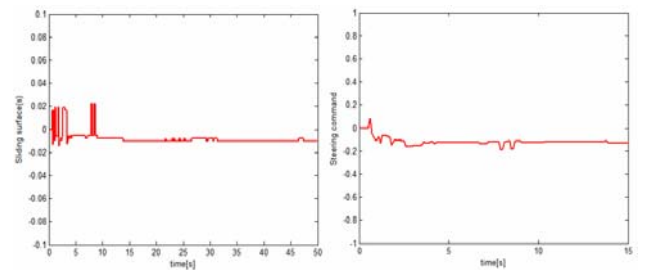


Fig. 12. Sliding surface (s) and the steering command (δ_f).

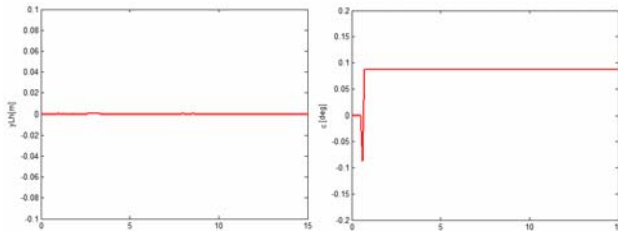


Fig. 13. Variation of the offset from the centerline at the look-ahead (y_{Lh}) and the angle between the tangent to the road and the vehicle orientation (ϵ_{Lh})

6. CONCLUSIONS

An SM controller based on the look-ahead reference system is employed in the feedback loop of the control system. Simulation example is used to evaluate the sliding-mode algorithm and to show the application of the algorithm in practice. The controller is simply structured and easy to implement.

From the simulation and real time results, it is concluded that the proposed strategy achieves the effectiveness of desired performance. In general, the primary objective of this research has been achieved where the proposed control system is able to track the centre of a lane automatically with small error under various conditions.

Future research lines include the experimental validation of our control scheme with the extension of our results to Four Driving-Steering Wheels steering mobile robots on more complex paths.

REFERENCES

- Abdullah, A.S., L.K. Hai, N.A.A. Osman, and M.Z. Zainon. (2006), Vision based automatic steering control using a PID controller, *Jurnal Teknologi*, 44(A), pp. 97-114.
- Danwei W. and Qi Feng. (2001), Trajectory planning for a four-wheel steering vehicle, *Proceedings of the IEEE International Conference on Robotics and Automation*, Seoul, pp. 3320-3325.
- Gao W. and J. C. Hung. (1993), Variable structure control of nonlinear systems: A new approach, *IEEE Trans. on Industrial Electronics*, 40(1), pp. 45-55.
- Hiraoka, T., O. Nishihara, and H. Kumamoto. (2009), Automatic path-tracking controller of a four-wheel steering vehicle, *Vehicle System Dynamics*, Taylor & Francis, 47(10), pp. 1205-1227.
- Huntsberger, T., H. Aghazarian, Y. Cheng, E. Baumgartner, E. Tunstel, C. Leger, A. Trebi-Ollennu, and P. Schenker. (2002), Rover Autonomy for Long Range Navigation and Science Data Acquisition on Planetary Surfaces, *Proceedings of the IEEE ICRA '02 Conference*, pp. 3161-3168.
- Lacaze, A., K. Murphy, and M. DelGiorno (2002), Autonomous Mobility for the DEMO III Experimental Unmanned Vehicles, *Proceedings of the AUVSI '02 Conference*, Orlando, USA.
- Montemerlo, M., S. Thrun, H. Dahlkamp, D. Stavens, and S. Strohband. (2006), Winning the DARPA Grand Challenge with an AI Robot, *Proceedings of the AAAI National Conference on Artificial Intelligence*, Boston, pp. 982-987.
- Seekur - Autonomous All-Weather Robot. Mobile Robots Inc. <http://www.mobilerobots.com/CommSeekur.html>.
- She, J-H., X. Xin, and Y. Ohyama. (2007). Estimation of equivalent input disturbance improves vehicular steering control, *IEEE Transactions on Vehicular Technology*, 56(6), pp. 3722-3731.
- Slotine J.J.E. and W. Li. (1991), *Applied nonlinear control*. Prentice-Hall, London.
- Solea, R., A. Filipescu, and G. Stamatescu. (2009a), Sliding-mode real-time mobile platform control in the presence of uncertainties, *Proceedings of the 48th IEEE Conference on Decision and Control and 28th Chinese Contr. Conf.*, Shanghai, pp. 7747-7752.
- Solea R. (2009b), *Sliding mode control applied in trajectory-tracking of WMRs and autonomous vehicles*, PhD Thesis, University of Coimbra, Portugal.
- Solea, R., A. Filipescu, and U. Nunes. (2009c), Sliding-mode control for trajectory-tracking of a wheeled mobile robot in presence of uncertainties, *Proceedings of the 7th Asian Control Conference*, Hong Kong, pp. 1701-1706.
- Utkin, V.I. (1992), Sliding modes in optimization and control, *Springer-Verlag*, New York.
- Utkin, V.I., J. Guldner, and J. Shi. (1999), *Sliding mode control in electromechanical systems*, Taylor & Francis, London.
- Wellington C. and A. Stentz. (2004), Online Adaptive Rough-Terrain Navigation in Vegetation. *Proceedings of the ICRA '04 Conference*. Vol. 1, pp. 96-101.